

Mesh phases of surfactant-water systems

V. A. Raghunathan

Abstract | Mesh phases are a class of intermediate phases found in many surfactant systems, which provide a topological link between the hexagonal phase made up of cylindrical micelles and the lamellar phase made up of planar bilayers. This article gives a brief review of the structures of these phases and also of different surfactant systems where they occur. The emphasis will be on a class of mixed surfactant systems in which mesh phases have been shown to occur recently. The influence of various structural parameters of the surfactant on the structure and stability of these phases is also discussed.

1. Introduction

Surfactants are amphiphilic molecules that self-assemble in water above a critical micellar concentration (CMC) to form aggregates called micelles¹. The formation of micelles is driven by the need to shield the hydrophobic part of the molecules from water. The CMC depends on the structure of the amphiphilic molecules, but typical values range from nM to mM. Micelles formed at concentrations just above CMC are generally almost spherical in shape, and contain typically about 50 molecules. This is especially true in the case of amphiphilic molecules containing a single hydrocarbon chain, such as sodium dodecylsulphate (SDS). These micelles are fairly monodisperse in size, since their radius is constrained to be comparable to the length of the surfactant molecule. As the concentration ϕ_s of the surfactant in the solution is increased, a sphere to rod transformation of the micellar shape takes place in many surfactant solutions. These rods elongate into cylindrical micelles as ϕ_s is further increased. The length of the cylindrical micelles is highly polydisperse; their radius is, of course, constrained to be comparable to the molecular length. The length distribution of these micelles is governed by the excess energy

needed to create their end caps. The end cap energy can be increased by the addition of certain salts and co-surfactants, such as short-chain alcohols. This results in a dramatic increase in the length of the micelles, leading to the formation of long worm-like micelles, whose behaviour resembles that of polymer solutions in many ways².

As ϕ_s is increased the cylindrical micelles come closer and form liquid crystalline phases characterized by long-range orientational ordering of these anisotropic aggregates. The first liquid crystalline phase to form is usually the hexagonal phase, where parallel cylindrical micelles are ordered on a two-dimensional hexagonal lattice. In a few cases a nematic liquid crystalline phase is found before the hexagonal phase, which has only short-range positional correlations. The hexagonal phase transforms into a lamellar phase at higher values of ϕ_s , which consists of a one-dimensional stack of surfactant bilayers separated by water. At very high surfactant concentrations an inverse hexagonal phase can form, consisting of water filled cylinders surrounded by the hydrophilic surfactant head groups, dispersed in the hydrocarbon matrix. Inverse cylindrical and spherical micelles can also form in some non-polar solvents.

2. Intermediate phases

As mentioned above, the hexagonal phase consists of cylindrical micelles with uniform curvature of the surfactant-water interface (neglecting the hemispherical end caps), whereas the lamellar phase is made up of planar bilayers. Many studies indicate that the morphological transformation from cylinders to bilayers does not take place abruptly, but through a sequence of intermediate shapes, giving rise to a sequence of so-called intermediate phases between the hexagonal and lamellar phases³. In ionic surfactants the intermediate phases usually occur only over very narrow ranges of composition. Further, the phase boundaries in these systems are almost independent of temperature. Therefore, detailed phase diagram studies are necessary to reveal their existence⁴.

Cubic phases

The first class of intermediate phases to be discovered are the bicontinuous cubic phases⁵. Their identification is made easier by the fact that they are optically isotropic, unlike all other phases found at comparable surfactant concentrations. Hence their formation can be easily visualized using polarizing optical microscopy observations. Cubic phases can be classified into two types. Type I cubic phases consist of two interpenetrating, topologically identical networks of cylindrical micelles, separated by water. In type II cubic phases two interpenetrating water channels are separated by a surfactant bilayer. Interestingly, the surface separating the two networks into two equal volumes can be described as a triply periodic minimal surface characterized by vanishing mean curvature everywhere on the surface. Three cubic structures have been reported belonging to the space groups $Im3m$, $Ia3d$ and $Pn3m$, usually associated with the P, gyroid and D triply periodic minimal surfaces, respectively. However, a given space group can be, in principle, realised by more than one triply periodic minimal surface⁶.

Although some bicontinuous noncubic intermediate phases have been proposed in the literature, their existence has not yet been unambiguously established³.

Ribbon phases

Another type of intermediate phase seen in some surfactants is the ribbon phase consisting of long micelles with roughly elliptical cross-section. These arrange on a two-dimensional rectangular lattice. Two types of structures have been reported, corresponding to the plane groups $cm\bar{m}$ and pgg .

Mesh phases

Mesh phases are the third type of intermediate phases seen in many surfactant systems. They consist of two-dimensional mesh-like aggregates, which can also be described as bilayers with a regular array of monodisperse pores. Mesh phases are of two types. In the ordered mesh phase the mesh-like aggregates lock into a three-dimensional lattice. On the other hand, the random mesh phase consists of a periodic stacking of these aggregates with no long-range positional correlations of the in-plane structure. All known structures of ordered mesh phases are either rhombohedral (space group: $R\bar{3}m$) or tetragonal (space group: $I4mm$). The former consists of a 3 layer stacking of 3-coordinated hexagonal mesh, whereas the latter has a 2-layer stacking of 4-coordinated square mesh.

The morphology of the surfactant aggregate is determined by the effective shape of the surfactant molecule, which can be described in terms of the surfactant shape parameter $p = v/al$, where v is the volume of the hydrocarbon chain, a the interfacial area per surfactant molecule, and l the chain length normal to the interface⁷. Spherical micelles are formed when $p = 1/3$, and cylindrical micelles when it is $1/2$. Planar bilayers are formed for $p = 1.0$. These ideas have been extended to other aggregate morphologies, assuming them to be homogeneous^{6,8}. It is found that mesh-like aggregates enclosing the chains occur for $1/2 < p < 2/3$, thus explaining their occurrence in between cylindrical micelles and planar bilayers.

3. Systems exhibiting mesh phases

Most of the studies on mesh phases have been carried out on the non-ionic surfactants, poly(oxyethylene glycol) alkyl ethers (C_nEO_m), where they occur over a rather wide range of composition⁹⁻¹⁷. The role of the length of the hydrocarbon chain of the surfactant in stabilizing different intermediate phases has been well studied in this class of surfactants. Shorter hydrocarbon chains are found to favor the bicontinuous cubic phase, whereas longer ones induce mesh phases¹⁶. Interestingly, all the ordered mesh phases seen in these systems have a rhombohedral structure belonging to the space group $R\bar{3}m$ ^{13,14,16}.

Mesh phases have also been seen in some anionic surfactants^{4,18-20}. A variety of intermediate phases, such as ribbon, ordered mesh and bicontinuous cubic, have been seen in the sodium dodecylsulphate

(SDS) — water system, albeit over very narrow ranges of composition⁴. The ordered mesh phase seen in this system has tetragonal symmetry (space group: $I4mm$), corresponding to a 2-layer stacking of 4-coordinated square mesh. On the other hand, mesh phases have been observed over wide composition ranges in aqueous solutions of some ionic surfactants with stiffer fluorocarbon chains^{18–20}. In these systems the structure of the mesh phase is found to depend critically on the type

of the counterion. For example, only a random mesh phase (L_{α}^D) is seen in cesium perfluorooctanoate (CsPFO), whereas its lithium counterpart shows an ordered tetragonal mesh phase in addition to the L_{α}^D phase. Further, the ordered mesh phase seen in tetramethylammonium perfluorodecanoate (TMAPFD) has a rhombohedral $R\bar{3}m$ structure. Above observations suggest that a balance between the aggregate flexibility, determined by the chain length or degree of fluorination, and the interfacial

Figure 1: Partial ternary phase diagram of the CTAB-SHN-water system at 30° C. The concentrations are in wt%. I, H, L_{α}^D and Int are the isotropic, hexagonal, random mesh and rhombohedral mesh phases, respectively. C denotes a multiphase region containing crystallites. The dashed line indicates mixtures with equimolar composition of CTAB and SHN.

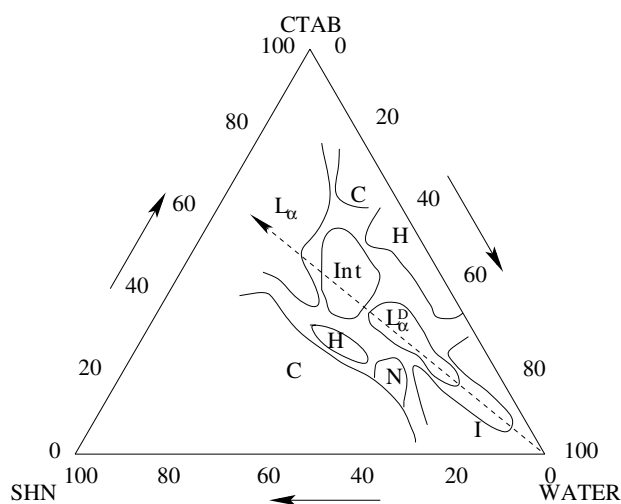
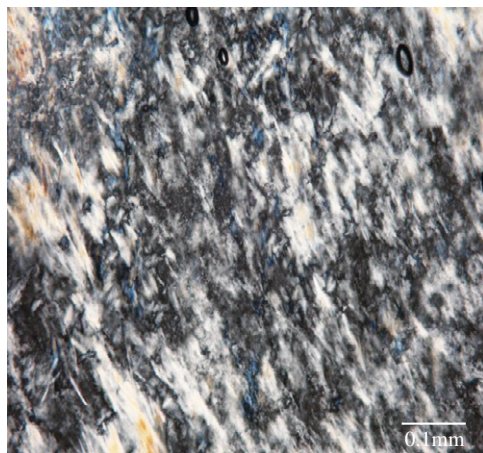


Figure 2: Polarizing optical microscopy texture of the hexagonal phase. Textures such as these are characteristic of each liquid crystalline phase, and hence they can often be used to identify the phase unambiguously.



curvature, determined by the head group size or the nature of the counterion, decides whether a bicontinuous cubic phase or a mesh phase is formed in a particular system³.

4. Mesh phases in mixed surfactant systems

Another class of surfactant systems exhibiting mesh phases has been recently introduced. It consists of a cationic surfactant, such as cetyltrimethylammonium bromide (CTAB) and

the organic salt sodium 3-hydroxy-2-naphthoate (SHN)^{21–23}. The hydroxy naphthoate counterion is known to bind strongly to CTAB micelles and lead to the formation of worm-like micelles in dilute solutions²⁴.

The ternary phase diagram of this system is shown in figure 1. A hexagonal phase occurs over a very wide range of water content in the CTAB-water binary system and a lamellar phase is found at very high values of ϕ_s ²⁵. The phase behaviour

Figure 3: Typical diffraction pattern of the hexagonal phase of surfactant solutions. Three peaks are seen with their scattering vectors in the ratio $1:\sqrt{3}:2$, corresponding to a two-dimensional hexagonal lattice. Higher order reflections are not usually seen in these systems due to the high degree of thermal disorder present in them.

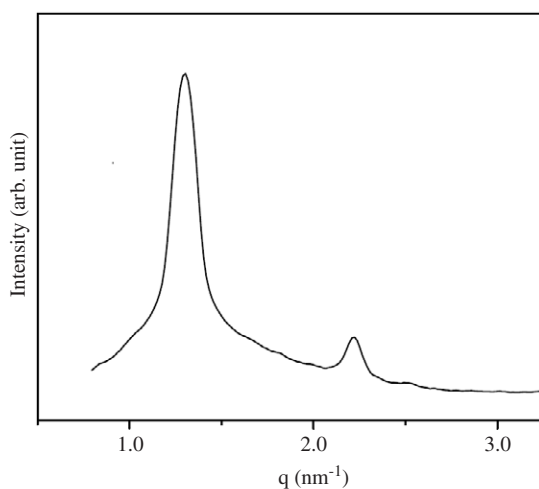


Figure 4: Temperature — concentration phase diagram of mixtures with equimolar composition of CTAB and SHN, where isotropic (I), random mesh (L_α^D), rhombohedral mesh (Int) and lamellar (L_α) phases are seen.

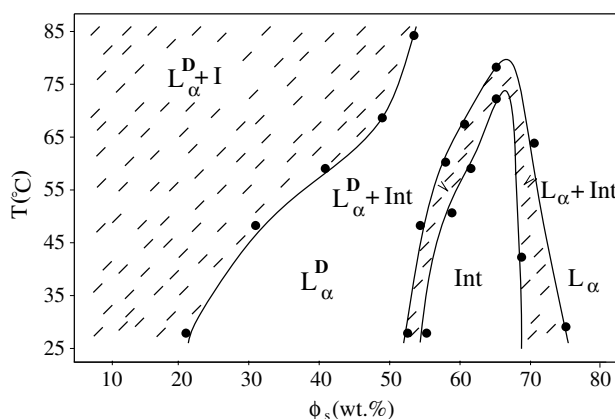


Figure 5: Polarizing optical microscopy texture of the random mesh phase. Since the symmetry of this phase is identical to that of the lamellar phase with planar bilayers, their textures are also identical. Therefore, the random mesh phase cannot be identified from its texture alone.

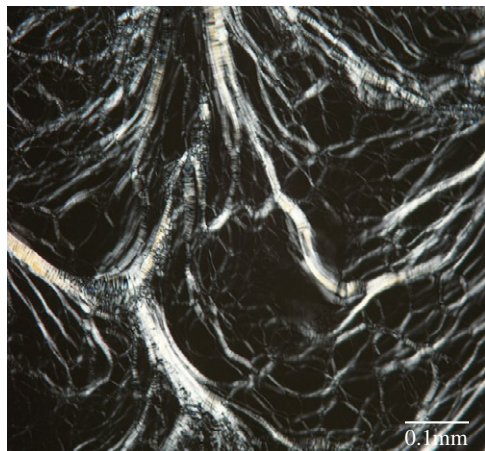
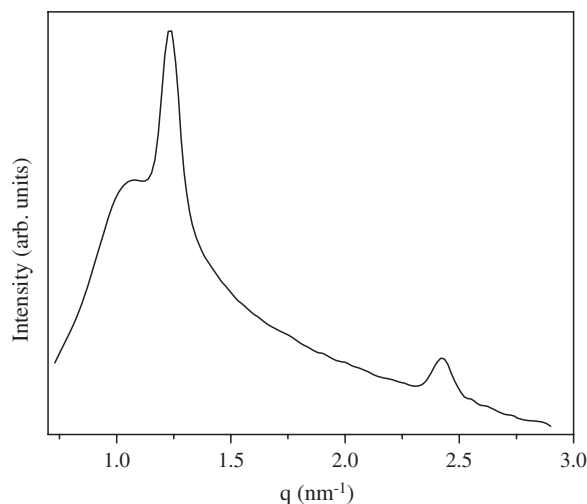


Figure 6: Diffraction pattern of an unoriented sample in the random mesh phase. Note the presence of the diffuse peak in the small angle region, in addition to the two sharp peaks arising from the lamellar periodicity.



remains essentially unchanged on the addition of small amounts of SHN. However, the isotropic phase of cylindrical micelles seen at high water content in the binary system is converted into a viscoelastic gel, which exhibits flow birefringence. This suggests the formation of worm-like micelles. Such behavior is quite common in ionic surfactants on the addition of simple inorganic as well as organic salts². NMR studies show that the organic part of strongly bound counterions, such as hydroxynaphthoate, penetrate the micellar aggregates projecting only their ionic

part into water²⁴. Such salts are found to be more efficient at producing worm-like micelles compared to simpler inorganic salts²⁶. The optical microscopy texture and diffraction pattern of the hexagonal phase seen at these compositions are shown in figures 2 and 3, respectively.

The phase behaviour is very different for mixtures with nearly equimolar compositions of CTAB and SHN (Figure 4). At these compositions the hexagonal phase is not observed. Instead, microscopy observations indicate the existence

Figure 7: Diffraction pattern of an oriented sample in the random mesh phase, with the layer normal aligned along z . Note that the diffuse peaks appear in the orthogonal direction, which indicates that they arise from in-plane structure of the layers. The contrast has been adjusted to show the splitting of the diffuse peaks along q_z due to the development of short-range positional correlations perpendicular to the layers. Such correlations arise on approaching the boundary with the ordered mesh phase.

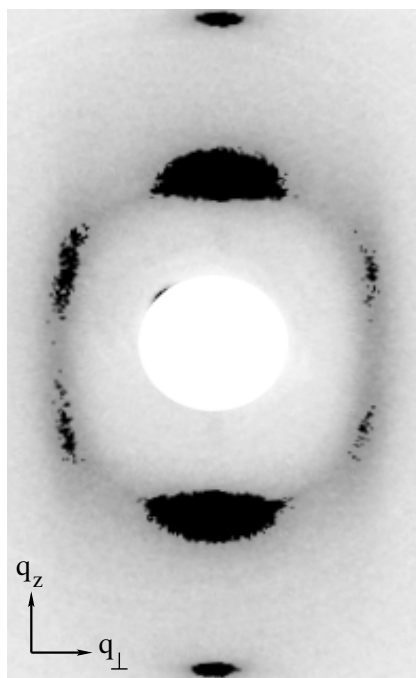
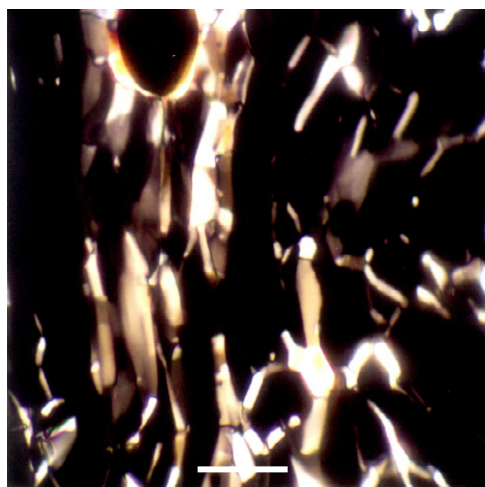


Figure 8: Polarizing optical microscopy texture of the ordered mesh phase in the CTAB-SHN-water system.



of a lamellar phase for ϕ_s ranging from about 25 to 50 wt% (Figure 5). At lower surfactant concentrations this phase coexists with an isotropic solution. However, x-ray diffraction patterns of

this phase show a diffuse peak in the small angle region, in addition to the set of peaks due to the lamellar stacking (Figure 6). Diffraction patterns of oriented samples show that the diffuse peaks

Figure 9: Diffraction pattern of an unaligned sample in the ordered mesh phase of the CTAB-SHN-water system. Only about 6 reflections are seen in these patterns due to the high degree of disorder present in these systems. This often makes an unambiguous determination of the structure of these phases difficult.

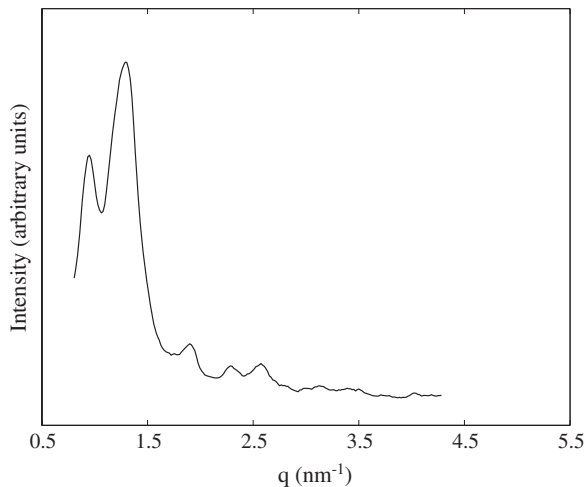
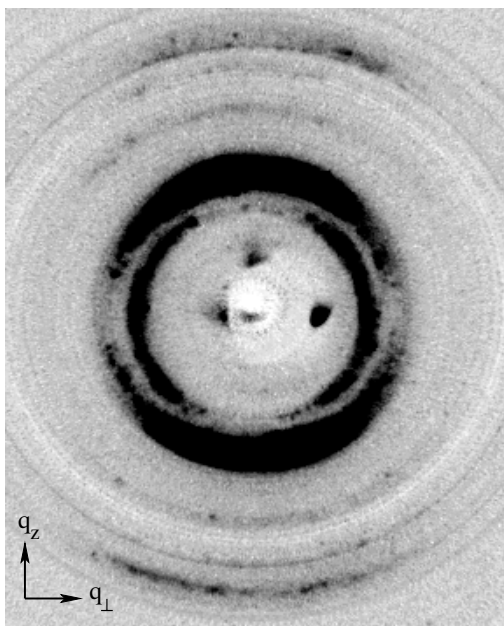


Figure 10: Diffraction pattern of a partially aligned sample in the ordered mesh phase of the CTAB-SHN-water system. Such patterns are very useful in ruling out alternative indexing schemes.



appear in a direction normal to the direction of layering, indicating that it arises from in-plane inhomogeneities with short-range positional correlations (Figure 7). Therefore, this phase can be tentatively identified as a random mesh phase, consisting of a stack of mesh-like aggregates with no long-range correlations of the in-plane structure.

At higher values of ϕ_s a mosaic texture is seen under the microscope, which is very different from those of the hexagonal and lamellar phases (Figure 8). Diffraction patterns of this phase show typically about 6 reflections, which do not correspond to either a lamellar or a two-dimensional hexagonal lattice (Figures 9 and 10). However,

Figure 11: Model for the rhombohedral mesh phase in the CTAB-SHN-water system corresponding to the space group $R\bar{3}m$, consisting of a 3-layer stacking of 3-coordinated hexagonal mesh-like aggregates.

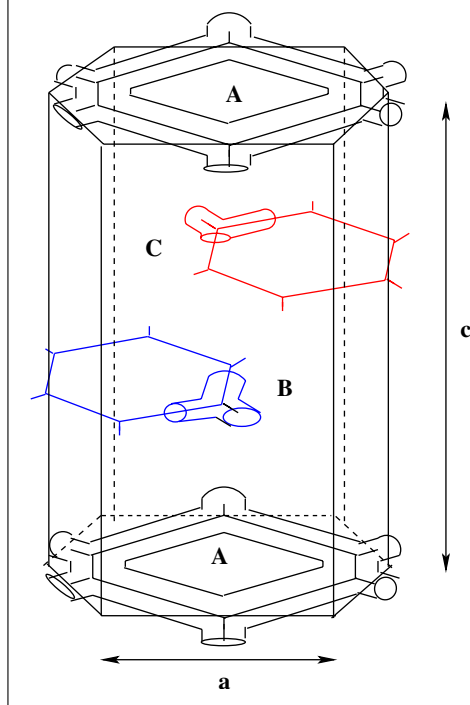
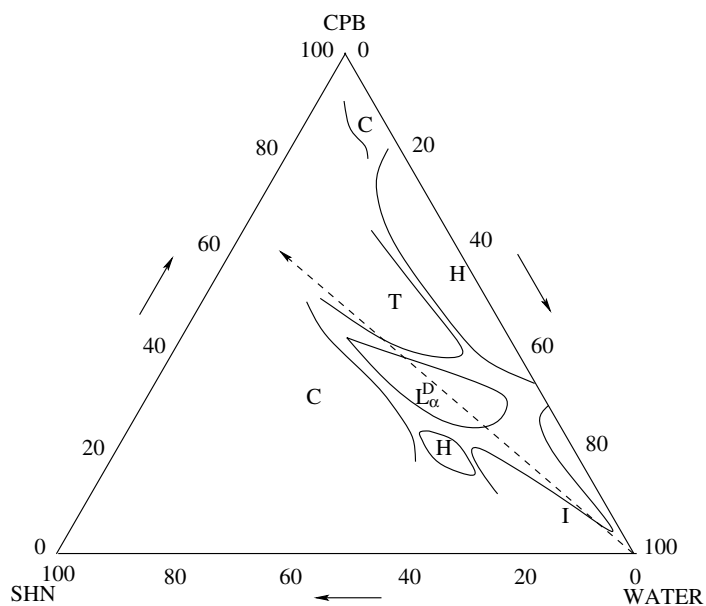


Figure 12: Partial ternary phase diagram of the CPB-SHN-water system at 30° C. The concentrations are in wt%. I , H , L_{α}^D and T are the isotropic, hexagonal, random mesh, and tetragonal mesh phases, respectively. C denotes a multiphase region containing crystallites. The dashed line indicates mixtures with equimolar composition of CPB and SHN.



these peaks can be indexed on a rhombohedral unit cell, corresponding to the space group $R\bar{3}m$. Interestingly, the value of the unit cell parameter c in this case is very close to $3d$, where d is the lamellar periodicity of the neighbouring random mesh phase. This suggests that the rhombohedral structure corresponds to a 3-layer stacking of the mesh-like aggregates. On the basis of these observations, a model can be proposed for the structure of this ordered mesh phase, consisting of a 3-layer stacking of 3-coordinated hexagonal mesh (Figure 11). As mentioned earlier, ordered mesh phases with a similar structure has been seen in other surfactant systems. The ordered mesh phase occurs up to $\phi_s \sim 75$ wt% in the equimolar mixtures, beyond which a

regular lamellar phase made up of planar bilayers is found.

The proposed model for the ordered mesh phase can be tested by checking if the radius of the cylindrical micelles estimated from it is comparable to the length of the surfactant molecule. Equating the surfactant volume fraction calculated from the model to its experimental value, the following expression for the radius r_m of the rod-like segments can be obtained¹²:

$$4(2 - \pi)r_m^3 + 2\pi ar_m^2 - a^2 d\phi_v = 0, \quad (1)$$

where $d = c/3$, a and c are the lattice parameters, and ϕ_v is the volume fraction of the surfactant.

Figure 13: Temperature — concentration phase diagram of mixtures with equimolar composition of CPB and SHN.

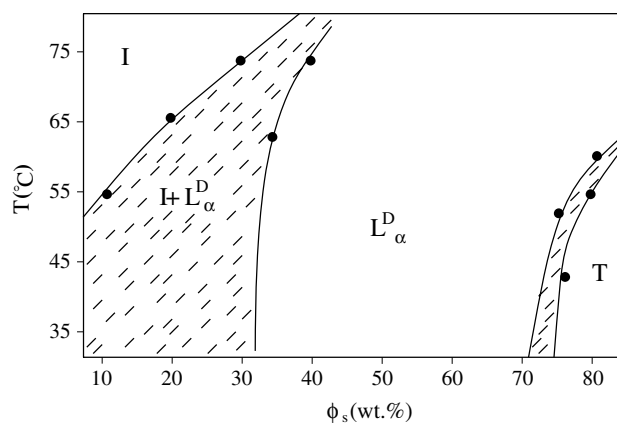


Figure 14: Typical polarizing optical microscopy texture of the tetragonal mesh phase of the CPB-SHN-water system.

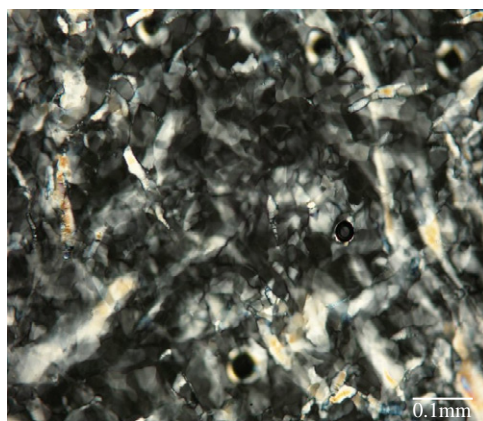


Figure 15: Diffraction pattern of a partially aligned sample in the tetragonal mesh phase.

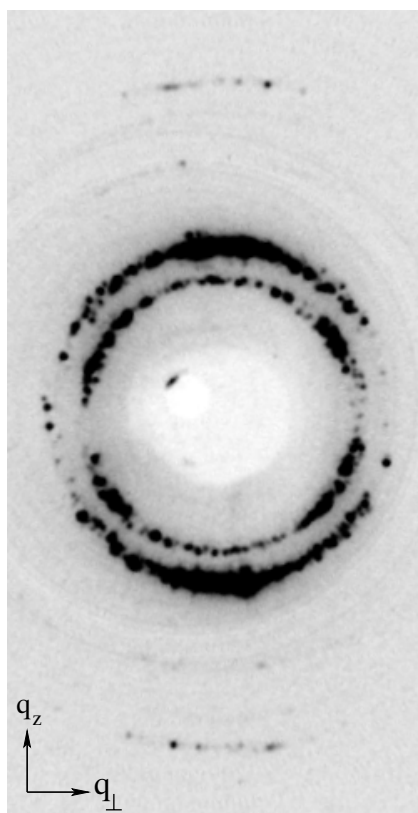
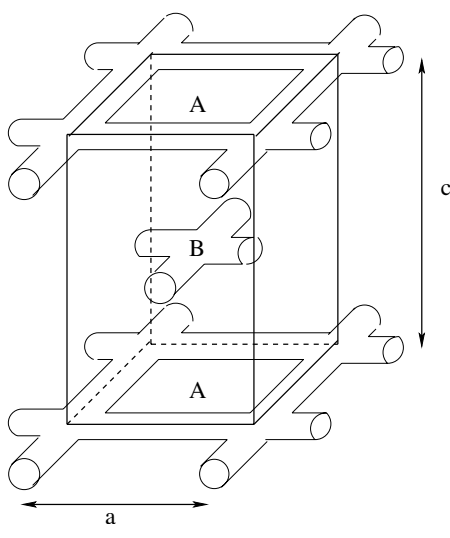


Figure 16: Model for the ordered mesh phase indicating the tetragonal unit cell.



Out of the 3 roots obtained for this cubic equation, only one turns out to be reasonable with the other two being either negative or unrealistically large.

Values of the micellar radius estimated using this expression are comparable to those reported in the literature for cylindrical micelles of CTAB, thus

Figure 17: Temperature — concentration phase diagram of mixtures with equimolar composition of DTAB and SHN.

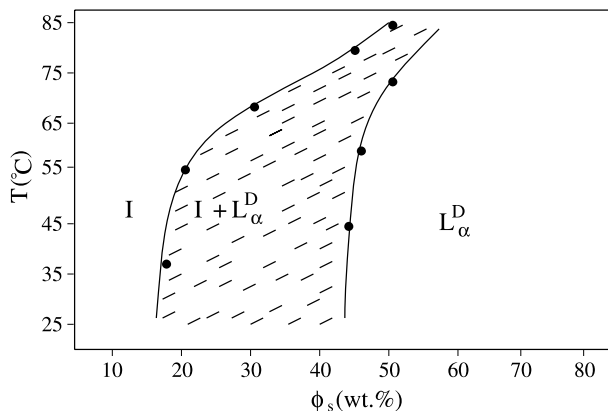
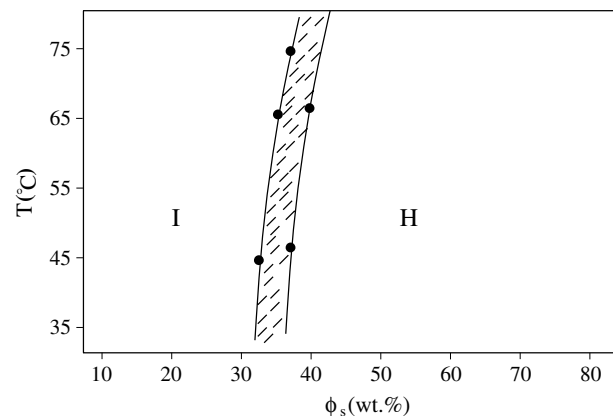


Figure 18: Temperature — composition phase diagram of mixtures with equimolar composition of CPB and SS.



giving additional validity to the proposed structure.

The above procedure can be extended to the random mesh phase by replacing d by the lamellar periodicity and a by the mesh size given by the diffuse peaks in the above relation. Again reasonable values of the micellar radius is obtained, indicating that this phase also consists of mesh-like aggregates, albeit without long-range positional correlations.

The ratio γ of the in-plane periodicity (given by the diffuse peak) to the lamellar periodicity is found to increase in the random mesh phase with increasing ϕ_s . The transition to the ordered mesh phase takes place when γ reaches a value of about 1.5. Similar observations have been reported in some other systems exhibiting the random mesh \rightarrow

ordered mesh transition²⁰. This behaviour can be understood in terms of the spatially modulated part of the interaction potential between the layers due to their mesh-like structure. It can be expected to decay exponentially with a decay length of the order of the in-plane periodicity¹. Hence it will be strong enough to lock the layers into a 3-dimensionally ordered structure only if the separation between adjacent layers is much less than the mesh-size, as observed.

At still higher SHN concentrations the mesh phases disappear and only nematic and hexagonal phases of cylindrical micelles are found. Phase behaviour at these compositions is, therefore, comparable to that found at low SHN

concentrations, making the ternary phase diagram somewhat symmetric about the equimolar CTAB-SHN composition. The analogous phase behavior at low and high SHN concentrations can be explained by the presence of highly charged aggregates at these compositions, although of opposite signs. Such phase behavior is quite common in mixtures of oppositely charged surfactants²⁷. Although SHN is not a surfactant, its effect on the phase behavior seems to be analogous to that of an anionic surfactant.

4.1. Influence of the surfactant headgroup

In order to determine the influence of the surfactant head group on the phase behaviour of these mixtures CTAB was replaced with cetylpyridinium bromide (CPB) which has the same chain length and counterion as CTAB. The overall phase behaviour of this system is very similar to that of the CTAB-SHN system (Figures 12 and 13). However, the structure of the ordered mesh phase seen in this system is different. The microscopy texture and diffraction pattern of this phase are shown in figures 14 and 15, respectively. The diffraction data can be indexed on a tetragonal lattice, corresponding to the space group $I4mm$.

As mentioned in the introduction, ordered mesh phases having tetragonal symmetry have been observed in other systems^{4,18} (Figure 16). The structure is made up of a square lattice of rods. In each unit, four cylindrical micelles meet at a node at right angles to each other to form a 2-D mesh-like layer. These layers are stacked with a two layer repeat with the centers of the squares in one layer placed on top of the nodes in the next. On dilution, the layers swell apart to form a lamellar structure and long-range positional correlations of the mesh structure are lost. Heating can also have a similar effect. Hence, the basic structural unit of the random mesh phase (L_{α}^D) and the ordered mesh phase can be expected to be the same.

As in the previous case, the proposed structure can be tested by comparing the value of the micellar radius obtained from it with those reported in the literature. Here too the calculated value is found to be comparable to the molecular length of the surfactant reported in the literature²⁸. The parameter γ , which is the ratio of the in-plane periodicity to the stacking periodicity, is found to increase with increasing ϕ_s in the random mesh phase of this system, as found in the earlier case.

Here the transition from the random to ordered mesh phase takes place when $\gamma \sim 1.6$, consistent with the transition being driven by the modulated part of the inter-layer interactions.

In place of the trimethylammonium head group in CTAB, CPB contains a pyridinium group. The observation of two different ordered mesh phases in these two systems suggests the critical role of inter-head group interactions in determining the structure of the mesh phase. Since these interactions determine the curvature of the surfactant-water interface, it is possible that small changes in them can favour one of these structures over the other, since the amount of curvature in the two structures is different. This behaviour is somewhat similar to that of perfluoroalkanoates, where Li^{+1} counterion leads to the formation of a tetragonal mesh phase, whereas TMA^{+1} counterion results in a rhombohedral mesh phase^{18,20}. An analogous situation also exists in the case of inverted mesh phases in anhydrous soaps, where the tetragonal structure is found for calcium counterions and the rhombohedral structure for strontium counterions²⁹. In all these situations small differences in the headgroup interactions — caused by changing the structure of the head groups in the present case, and by varying the counterions in the other two — result in different structures of the ordered mesh phase.

4.2. Influence of the chain length

The length of the hydrocarbon chain of the surfactant is an important parameter determining the stability of mesh phases. This is believed to be related to the flexibility of the micelles since fluorination of the chains is found to have the same effect as making them longer. In order to check the influence of this parameter on the phase behaviour CTAB was replaced in the mixtures with its shorter chain analogue dodecyltrimethylammonium bromide (DTAB). The phase diagram of equimolar mixtures of DTAB and SHN is presented in figure 17. For $\phi_s < 45$ wt%, the lamellar phase coexists with an isotropic phase. At $\phi_s = 50$ wt%, in addition to the lamellar peaks a diffuse peak is observed in the diffraction pattern, indicating the presence of a random mesh phase. The average defect separation decreases on increasing ϕ_s , similar to the trend observed in the random mesh phase of the cesium perfluorooctanoate — water system¹⁹. However, an ordered mesh phase is not observed in this system

over the range of water content and temperature studied.

The random mesh phase of DTAB-SHN was also modeled based on the structure proposed for that of CTAB-SHN. The radius of the cylinders estimated from the model is found to decrease slightly on increasing ϕ_s . The estimated radius of DTAB micelles is also comparable with the values quoted in the literature. The absence of the intermediate phase in the DTAB-SHN-water system is consistent with observations in some nonionic surfactant systems, where decreasing the alkyl chain length destabilizes the ordered mesh phase. However, in nonionic surfactant systems the intermediate mesh phase is usually replaced by a cubic phase on decreasing the chain length^{11–13,16}. But in the present system no cubic phase is observed, and the random mesh phase occurs over a very wide range of water content.

In the DTAB-SHN system the parameter γ is found to decrease with increasing surfactant content; a trend opposite to that seen in the CTAB-SHN and CPB-SHN systems. In the latter systems an ordered mesh phase is formed when γ exceeds 1.5. In the case of DTAB, γ is always much less than this critical value, and hence it is possible that the interlayer interactions are not strong enough to lock them into a 3-dimensional lattice. However, the reason for the opposite trend seen on decreasing the chain length remains unclear.

4.3. Influence of the strongly bound counterion

In order to check the influence of the strongly bound counterion on the phase behaviour SHN was replaced in the solution with other organic salts, such as sodium salicylate (SS) and sodium tosylate (ST). Both these systems were found to behave very differently from the mixtures containing SHN. The phase diagram of mixtures with equimolar composition of CPB and SS is shown in figure 18). At low ϕ_s , there is an isotropic gel. The phase diagram is dominated by the presence of the 2-D hexagonal phase at higher concentrations. No other liquid crystalline phases are observed in this system up to a ϕ_s of 80 wt%, and the phase diagram is quite similar to that of the CPB-water binary system. The phase behaviour of CPB-ST mixtures is almost identical.

The addition of salt to a dilute ionic surfactant solution is well known to induce the formation of long worm-like micelles, as found here for SS, ST and for low concentrations of SHN. Both SS and ST,

which contain a benzene ring, do not change the cylindrical morphology of CPB micelles, other than making them longer. SHN containing a naphthalene group is found to transform the cylindrical micelles into mesh-like aggregates. It is not clear if this difference in the phase behaviour between SHN on the one hand, and SS and ST on the other, is just related to differences in their size, or if other factors, such as their hydrophobicity, are also involved.

5. Conclusion

Random and ordered mesh phases have been observed in a variety of surfactant systems, in between the hexagonal and lamellar phases. The structure and stability of the mesh phases are found to be very sensitive to the inter-headgroup interactions, which can be tuned, in the case of ionic surfactants, by changing either the surfactant head group or the counterion. Interestingly, all known structures of ordered mesh phases are either rhombohedral (space group $R\bar{3}m$) or tetragonal (space group $I4mm$). Detailed studies of the energetics of these systems are needed to understand why these structures are favoured over other possibilities.

Received 08 August 2008; revised 26 August 2008.

References

1. Israelachvili, J. *Intermolecular and Surface Forces*, 2nd edition, Academic Press, London, 1991.
2. Cates, M. E.; Candau, S. J. *J. Phys. Condens. Matter* 1990, 2, 6869.
3. Holmes, M. C.; Leaver, M. S. in *Bicontinuous liquid crystals*; Lynch, M. L., Spicer, P. T., Eds.; Surfactant Science Series, Volume 127, CRC Press: Boca Raton, FL, 2005; pp 15–39.
4. Kékicheff, P.; Cabane, B. *J. Phys.* 1987, 48, 1571.
5. Luzzati, V. In *Biological Membrane*; Chapman, D. Eds.; Academic Press: London and New York, p71, 1968.
6. Hyde, S. T. *Pure Appl. Chem.* 1992, 64, 1617.
7. Israelachvili, J. N.; Mitchell, D. J.; Ninham, B. W. *J. Chem. Soc. Faraday Trans. 2* 1976, 72, 1525.
8. Hyde, S. T. *J. de Phys.* 1990, C7, 209.
9. Funari, S.S.; Holmes, M.C.; Tiddy, G. J. T. *J. Phys. Chem.* 1992, 96, 11029.
10. Funari, S.S.; Holmes, M.C.; Tiddy, G. J. T. *J. Phys. Chem.* 1994, 98, 3015.
11. Burgoyne, J.; Holmes, M. C.; Tiddy, G. J. T. *J. Phys. Chem.* 1995, 99, 6054.
12. Fairhurst, C.E.; Holmes, M.C.; Leaver, M.S. *Langmuir* 1997, 13, 4964.
13. Funari, S.S.; Rapp, G. *Proc. Natl. Acad. Sci. USA* 1999, 96, 7756.
14. Leaver, M.; Fogden, A.; Holmes, M.; Fairhurst, C. *Langmuir* 2001, 17, 35.
15. Imai, M.; Nakaya, K.; Kawakatsu, T.; Seto, H. *J. Chem. Phys.* 2003, 119, 8103.

16. Imai, M.; Sakai, K.; Kikuchi, M.; Nakaya, K.; Saeki, A.; Teramoto, T. *J. Chem. Phys.* 2005, 122, 214906.
17. Baciú, M.; Olsson, U.; Leaver, M. S.; Holmes, M.C. *J. Phys. Chem. B* 2006, 110, 8184.
18. Kékicheff, P.; Tiddy, G. J. T. *J. Phys. Chem.* 1989, 93, 2520.
19. Leaver, M.S.; Holmes, M.C. *J. Phys. II France*, 1993 3, 105.
20. Puntambekar, S.; Holmes, M. C.; Lever, M. S. *Liq. Cryst.* 2000, 27, 743.
21. Krishnaswamy, R.; Ghosh, S. K.; Lakshmanan, S.; Raghunathan, V. A.; Sood, A. K. *Langmuir* 2005, 21, 10439.
22. Ghosh, S. K.; Ganapathy, R.; Krishnaswamy, R.; Bellare, J.; Raghunathan, V. A.; Sood, A. K. *Langmuir* 2007, 23, 3606.
23. Ghosh, S. K.; V. A. Raghunathan (to be published).
24. Mishra, B. K.; Samant, S. D.; Pradhan, P.; Mishra, S. B.; Manohar, C. *Langmuir* 1993, 9, 894.
25. Auray, X.; Petipas, C.; Anthore, R.; Rico, I.; Lattes, A. *J. Phys. Chem* 1989, 93, 7458.
26. Garg, G.; Hassan, P. A.; Aswal, V. K.; Kulshrestha, S. K. *J. Phys. Chem. B* 2005, 109, 1340.
27. Kaler, E. W.; Herrington, K. L.; Murthy, A. K.; Zasadzinski, J. A. N. *J. Phys. Chem.* 1992, 96, 6698 .
28. Reiss-Husson, F.; Luzzati, V. *J. Phys. Chem.* 1964, 68, 3504.
29. Luzzati, V.; Tardieu, A.; Gulik-Krzwicki, T. *Nature* 1968, 217, 1028.



V. A. Raghunathan is an associate professor at the Raman Research Institute, Bangalore. He obtained his M.Sc degree in Physics from Bangalore university and his Ph.D work was done at the Raman Research Institute. His research interests are in the physics of soft condensed matter and biological systems.